Preparation, Characterization, and Application of Graphene−Zinc Oxide Composites (G−ZnO) for the Adsorption of Cu(II), Pb(II), and Cr(III)

ARTICLE *in* JOURNAL OF CHEMICAL & ENGINEERING DATA · AUGUST 2013

Impact Factor: 2.04 · DOI: 10.1021/je400384z

4 AUTHORS, INCLUDING:

Zhao Xiaowei
Tianjin University of Technology
12 PUBLICATIONS **217** CITATIONS

SEE PROFILE

Qiong Jia
Jilin University
98 PUBLICATIONS **1,085** CITATIONS

SEE PROFILE

Journal of chemical & engineering data

Article

pubs.acs.org/jced

Preparation, Characterization, and Application of Graphene−Zinc Oxide Composites (G−ZnO) for the Adsorption of Cu(II), Pb(II), and Cr(III)

Xiaowei Zhao,[†] Bin Hu,[‡] Juanjuan Ye,[†] and Qiong Jia*[,†]

[†]College of Chemistry and [‡]State Key Laboratory of Inorganic Synthesis and Preparative Chemistry, College of Chemistry, Jilin University, Changchun, 130012, China

ABSTRACT: In the present study, graphene−zinc oxide composites (G−ZnO) were prepared and applied to the adsorption of Cu(II), Pb(II), and Cr(III) from aqueous solutions. The synthesized composites were characterized by X-ray diffraction and transmission electron microscopy. Effects of pH and contact time were studied in batch experiments. Kinetics, adsorption isotherms, and thermodynamics were also examined. Kinetics experiments indicated that the processes could be simulated by a pseudo-second-order model. The experimental results of equilibrium adsorption were tested by Langmuir and Freundlich isotherms, indicating that the former fit the data better. Thermodynamic parameters, the Gibbs free energy change (ΔG), enthalpy change (ΔH), and entropy change (ΔS), were calculated, indicating that the adsorption of heavy metals onto G−ZnO was spontaneous and endothermic in nature.

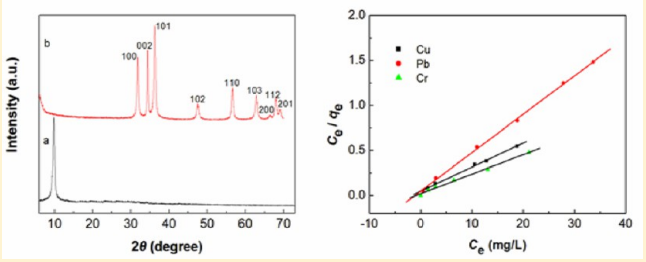

1. INTRODUCTION

Water pollution caused by heavy metals has become a serious environmental issue. Even at low concentrations, heavy metals have toxic effects and can accumulate along the food chain, leading to serious ecological and health hazards. Therefore, it is important to eliminate hazardous heavy metals in wastewater before discharging them into the ecosystem. Over the past years, various methods have been applied to remove heavy metals from aqueous media including chemical precipitation,[1,2] membrane processes,[3,4] ion exchange,[5] and adsorption.[6−11] Among these methods, adsorption strategy is considered as one of the most economical and efficient techniques because of its advantages such as simple design and facile handling. Various materials have been employed as effective adsorbents, e.g., activated carbon,[6] modified silica gel,[7] inorganic materials,[8,9] and sorption resins.[10−13]

In recent years, nanometer-sized materials have attracted growing attention because of their unique physical and chemical properties.[14,15] Nanometer-sized metal oxides exhibit intrinsic surface reactivities and large surface areas, therefore, they can strongly adsorb many substances including trace metals. From the literature survey, various nanometer-sized metal oxides have been synthesized and applied as the adsorbent for the preconcentration of trace metals.[16−20] However, because of the fine grain size, when a suspension of nanometer-sized metal oxide is employed for the adsorption of metal ions, the grains aggregate easily, which results in decreased activities. To overcome this technical bottleneck, some researchers immobilized nanometer-sized metal oxides on different substrates such as activated carbon (AC)[21,22] and carbon nanotubes (CNTs).[23−27] For example, Machida et al.[21] prepared AC-supported zinc oxide and used this composite for the effective adsorption of Pb(II). Chen et al.[23] indicated that CNTs−iron oxides magnetic composites could be employed as an effective adsorbent for the adsorption of Ni(II) and Sr(II) from wastewater. The adsorption capacity of the composites was determined to be much higher than that of iron oxides. Therefore, the choice of suitable supporting materials is of particular importance.

Graphene, a new member of the carbon family, is regarded to be one of the most promising materials.[28] Graphene-based materials such as graphene and chemically modified graphene have found many applications in many areas. Recent literatures suggest that reduced graphene oxide-supported materials have higher binding capacities than free nanometer-sized materials.[29] Graphene possesses similar physical properties to CNTs but has larger surface areas than the latter. Moreover, the cost of graphene is much lower than that of CNTs when they are produced in large quantities.[30,31] Therefore, graphene has the potential to be employed as a low-cost alternative for supporting materials.

Herein, the main objective of the current study is to immobilize nanostructured zinc oxide on graphene and apply the synthesized graphene−zinc oxide composites (G−ZnO) to the adsorption of Cu(II), Pb(II), and Cr(III) ions. Zinc oxide is employed because it is an environmental friendly material. As an adsorbent, however, ZnO is mostly applied to the removal of H_2S.[32] Recently, ZnO was successfully applied to the preconcentration of trace metal ions by Wang et al.[33] This work not only demonstrated the

Received: December 23, 2012
Accepted: June 10, 2013
Published: August 5, 2013

possibility and validity of G−ZnO composites as promising adsorbents for contaminant removal and environmental remediation, but also gave insight into understanding the adsorptive behavior of G−ZnO composites.

2. MATERIALS AND METHODS

2.1. Chemicals. All chemicals used were of analytical grade. $CuCl_2{\cdot}2H_2O$, $PbCl_2$, and $CrCl_3{\cdot}6H_2O$ were obtained from Tianjin Guangfu Chemical Plant (Tianjin, China). Stock solutions (1000 μg mL^{-1}) of Cu(II), Pb(II), and Cr(III) were prepared by dissolving $CuCl_2{\cdot}2H_2O$, $PbCl_2$, and $CrCl_3{\cdot}6H_2O$ in deionized water, respectively. The working solutions were daily prepared by stepwise dilution of the stock solutions. 0.1 mol L^{-1} HCl and 0.1 mol L^{-1} $NH_3{\cdot}H_2O$ were used to adjust pH values.

2.2. Instruments. The concentration of the three metal ions was determined by flame atomic absorption spectrometer (FAAS) made by Beijing Purkinje General Instruments Co., Ltd. (Beijing, China) equipped with an air−acetylene flame. The flow rates of air and acetylene were 10 L min^{-1} and 2 L min^{-1}, respectively. The wavelengths used for Cu(II), Pb(II), and Cr(III) were (324.8, 283.3, and 357.9) nm. X-ray diffraction (XRD) determinations were performed by a D-500 diffractometer (Siemens, Germany) with a nickel-filtered Cu Kα radiation in the 2θ diffraction angle range extending from 5° to 75°. The intensity values were read at $\Delta(2\theta)$ intervals of 0.02° with a step time of 1.2 s. The structure and morphology of the as-obtained products were observed by a transmission electron microscope made by JEOL Ltd. (Tokyo, Japan).

2.3. Preparation of Graphene−Zinc Oxide Composites (G−ZnO). Unless otherwise stated, all chemicals were obtained from Beijing Chemical Works (Beijing China). First, graphite oxide (GO) was prepared by a modified Hummers method.[34,35] Briefly, 5.0 g of graphite powder (Sinopharm Chemical Reagent Co., Ltd., Shanghai, China) was added into a beak containing 120 mL of concentrated H_2SO_4 and 2.5 g of $NaNO_3$ at 0 °C. When vigorous stirring was maintained, 15.0 g of $KMnO_4$ was slowly added, and the temperature was kept below 15 °C. After the mixture was stirred at 35 °C to be pasty brownish, it was diluted with deionized water. A 10 mL portion of H_2O_2 (100 w = 30) solution was slowly added until the color of the mixture became bright yellow. Finally, the mixture was filtered and washed with 5 % HCl (v/v) aqueous solution to remove metal ions followed by 1.0 L deionized water to remove the acid. Finally, the as-received solid was dried at 60 °C for 24 h.[35]

Graphene−zinc oxide composites (G−ZnO) with four different ZnO loading levels were synthesized as follows. The above-obtained GO was dissolved in 40 mL of ethylene glycol and sonicated for 1 h under ambient condition. A brown dispersion was thus obtained and then zinc acetate ($ZnC_4H_6O_4{\cdot}2H_2O$) dissolved in ethylene glycol was added under magnetic stirring. Subsequently, a predetermined amount of NaOH solution was added to the mixture. After being stirred for 30 min, the mixture was transferred into a Teflon-lined stainless steel autoclave and allowed to react for 24 h at 160 °C. The prepared composites were then centrifuged and washed by absolute ethanol and deionized water for several times. The product was dried in a vacuum oven for 24 h at 60 °C.[36]

2.4. Batch Adsorption Experiments. The adsorption studies were conducted using batch experiments. Amounts of 0.02 g of adsorbent and 20 mL of solution containing the metal ions were added into special glass-stoppered tubes, and the mixture was shaken at 20 ± 1 °C for a period of time. The initial metal concentrations were fixed at 10 mg L^{-1} unless otherwise stated. At certain aqueous pH values (2.0 to 7.0) and contact time (10 min to 120 min), the adsorption behaviors of the metal ions were investigated. After the sorption reached equilibrium, the suspension was filtered through 0.45 μm filters. The metal concentration in the aqueous phase was determined by FAAS. All the adsorption experiments were conducted in triplicate, and the results were averaged. The adsorption percentage was obtained with eq 1 and the adsorption capacity was calculated with eq 2.

$$\text{adsorption}\ (\%) = \frac{C_0 - C_e}{C_0}100 \quad (1)$$

$$q_e = \frac{(C_0 - C_e)V}{m} \quad (2)$$

where C_0 and C_e denote the initial and equilibrium metal ion concentrations (mg L^{-1}), respectively; V represents the volume of the metal ion solution (mL); m means the amount of adsorbent (mg).

3. RESULTS AND DISCUSSION

3.1. Characterization of G−ZnO Composites. X-ray diffraction (XRD) measurements were carried out to investigate the phase and structure of the synthesized composites. The typical XRD patterns of the GO and G−ZnO composites (ZnO loading level: 100 w = 20) were shown in Figure 1. As can be

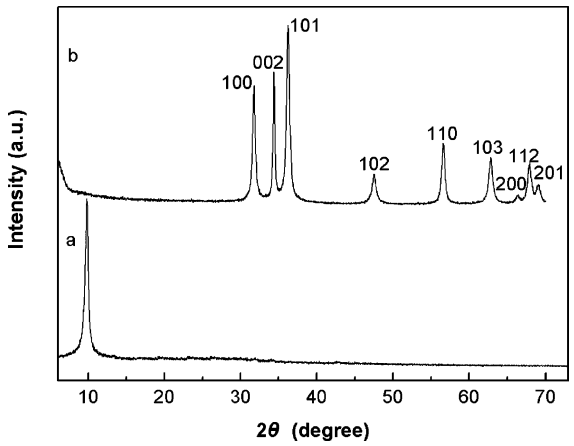

Figure 1. XRD patterns of GO (a) and G−ZnO composites (b).

observed from Figure 1a, the XRD pattern of the synthesized GO shows a sharp peak at 2θ = 10.6°, corresponding to the (001) reflection of GO.[37] From Figure 1b, all the diffraction peaks of the G−ZnO composites (ZnO loading level: 100 w = 20) synthesized can be subjected to hexagonal ZnO (JCPDS 36-1451). However, there are not characteristic peaks assigned to graphene oxide or graphite (the characteristic peak at around 2θ = 26.5°) in G−ZnO composites, indicating that GO was simultaneously reduced to graphene by the ethylene glycol at high temperature during the formation of ZnO nanoparticles, and the produced graphene sheets were hard to aggregate back to graphite due to the existence of ZnO nanoparticles on graphene sheets surface.[38]

The morphology and structure of the as-synthesized GO and all the G−ZnO composites were further investigated by TEM determinations. As a representative, the TEM images of the as-synthesized GO and the G−ZnO composites (ZnO loading

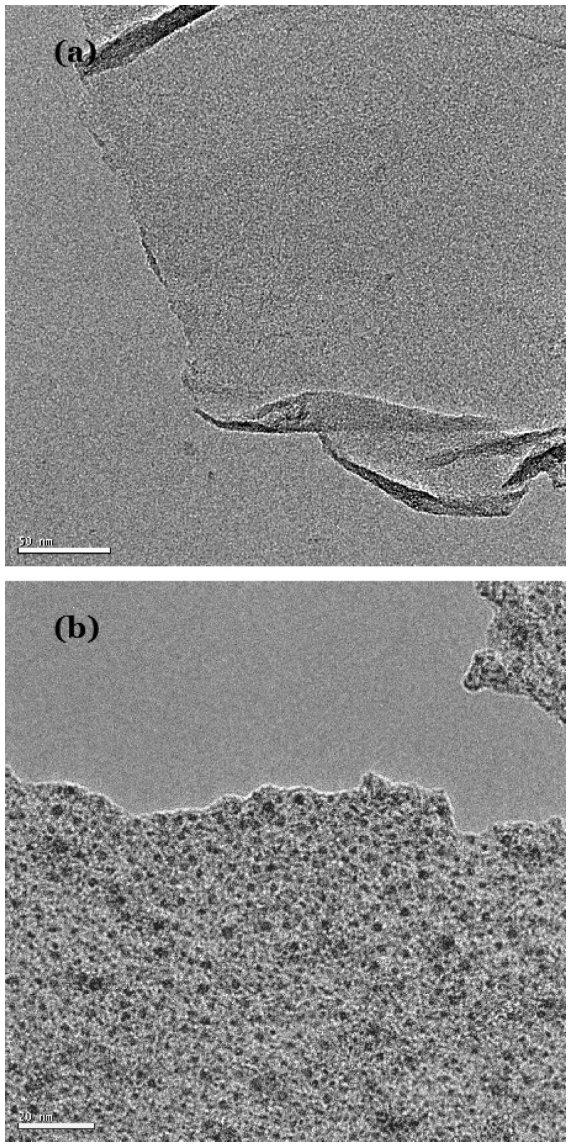

Figure 2. TEM images of GO (a) and G−ZnO composites (b).

level of 100 w = 20) were presented in Figure 2. The as-synthesized GO consists of very thin carbon flakes (Figure 2a). The wrinkling of the GO is attributed to point or line defects formed upon exfoliation or present in areas of a few intact epoxide groups.[39] In the case of the G−ZnO composites (ZnO loading level of 100 w = 20) (Figure 2b), it is obvious that graphene is well decorated by ZnO nanoparticles. In addition, almost no ZnO nanoparticles were found outside graphene.

3.2. Effect of ZnO Loading Level. The effect of ZnO loading level on the adsorption capacity was investigated using Cu(II) as representative. Results revealed that the adsorption percentage of Cu(II) increased from 90.27 % to 96.56 % with increasing ZnO loading amount from 100 w = (10 to 20). The most effective removal of Cu(II) occurs at the ZnO loading level of 100 w = 20. The decrease in adsorption percentage with further increase in the ZnO loading level (the adsorption percentage was determined as 92.13 % and 86.73 % for 100 w = (30 and 50) ZnO loading level, respectively) may be because of the aggregation of ZnO nanoparticles, which leads to unwanted reduction in the active surface area. The adsorbent with ZnO loading level of 100 w = 20 was selected in this study.

3.3. Effect of pH. The solution pH is a very important parameter which affects the adsorption process. In this study, the adsorption experiments were carried out within the initial pH range of 2.0 to 7.0 when other conditions were fixed, that is, adsorbent dosage as 0.2 g, metal ion concentration as 10 mg L^{-1}, and contact time as 120 min. Results were presented in Figure 3. Under the present experimental conditions, the adsorption

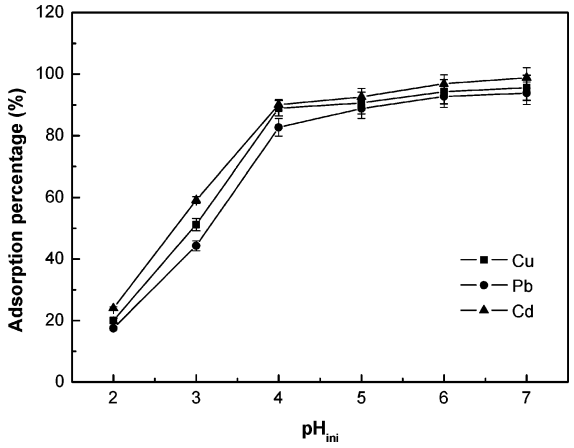

Figure 3. Effect of solution pH on the adsorption of Cu(II), Pb(II), and Cr(II) onto G−ZnO composites. Dosage of adsorbent = 0.02 g, concentration of metal ions = 10 mg L^{-1}, contact time = 120 min.

percentage increases sharply in the pH range of 2.0 to 4.0 but increases slightly with when the pH value rises from 4.0 to 7.0. Similar results were also reported in some previous papers for metal ions adsorption with different adsorbents.[8,21] Because of compromising quantitative adsorption and precipitation at high pH values, a sample pH of 6.0 was chosen as optimum for further studies.

3.4. Effect of Contact Time. The effect of contact time on the adsorption of metal ions was studied by adding 0.02 g of adsorbent and 20.0 mL of sample solution into special glass-stoppered tubes. The tubes were shaken for different time intervals in a temperature-controlled shaker. When other conditions were fixed (adsorbent dosage as 0.2 g, metal ion concentration as 10 mg L^{-1}, and pH$_{ini}$ as 6.0), the experiments were performed when the contact time varied from 10 to 120 min. Results were shown in Figure 4. It is evident that the adsorption of metal ions

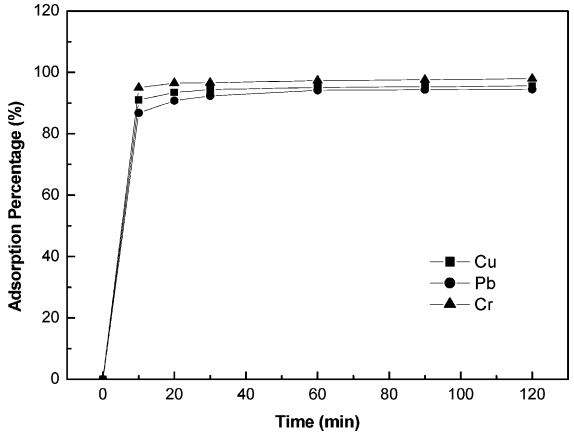

Figure 4. Effect of contact time on the adsorption of Cu(II), Pb(II), and Cr(III) onto G−ZnO composites. Dosage of adsorbent = 0.02 g, concentration of metal ions = 10 mg L^{-1}, pH = 6.0.

dx.doi.org/10.1021/je400384z | J. Chem. Eng. Data 2013, 58, 2395−2401

on G−ZnO composites is initially very fast. In the present work, 120 min was selected as the contact time to ensure equilibrium.

3.5. Adsorption Kinetics. Sorption kinetics is an important aspect of the operation defining the efficiency of the process. It is expressed in terms of the rate of solute removal that controls the residence time of the adsorbate in the solid−solution interface. In general, pseudo-first-order and pseudo-second-order models are used for kinetic studies.

The linearized form of pseudo-first-order rate equation is given as eq 3,

$$\log(q_e - q_t) = \log q_e - \frac{k_1}{2.303}t \quad (3)$$

where q_t and q_e are the amounts of metal ions adsorbed at time t and at equilibrium (mg g^{-1}), respectively, k_1 is the rate constant of pseudo-first-order adsorption process (min^{-1}).

On the other hand, the experimental data were also applied to the pseudo-second-order kinetic model (Figure 5) given as eq 4,

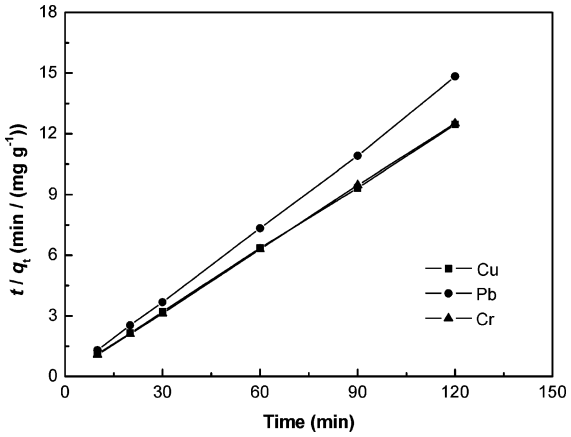

Figure 5. Pseudo-second-order kinetics plots for the adsorption of Cu(II), Pb(II), and Cr(III) onto G−ZnO composites. Dosage of adsorbent = 0.02 g, concentration of metal ions = 10 mg L^{-1}, contact time = 120 min, pH = 6.0.

$$\frac{t}{q_t} = \frac{1}{k_2 q_e^2} + \frac{1}{q_e}t \quad (4)$$

where k_2 is the rate constant of the pseudo-second-order sorption (g mg^{-1} min^{-1}) and q_e and q_t are defined as the same as above.

The calculated parameters from two kinetic models were listed in Table 1. The pseudo-second-order equation provides the better correlation coefficient and agreement between calculated q_e values and the experimental data. However, the pseudo-first-order equation cannot give a good fit to the experimental data. The correlation coefficient values of pseudo-second-order model are much higher than those of pseudo-first-order model, indicating that the chemical adsorption can be well described with the pseudo-second-order kinetic model.[40]

3.6. Adsorption Isotherms. The equilibrium adsorption isotherm was investigated because it is important not only for describing the interactive behavior between adsorbate and adsorbent, but also for designing adsorption systems. In these studies, the adsorption data were studied by Langmuir and Freundlich isotherm models when the initial metal ion concentrations ranged from 10 to 60 mg L^{-1}.

The Langmuir isotherm assumes that adsorption occurs at specific homogeneous sites within the adsorbent. There are no subsequent interactions among the adsorbed molecules. The expression for the Langmuir isotherm is

$$\frac{C_e}{q_e} = \frac{1}{q_{max}b} + \frac{C_e}{q_{max}} \quad (5)$$

where q_e and C_e are the adsorption capacity (mg g^{-1}) and the equilibrium concentration of the adsorbate (mg L^{-1}), respectively, q_{max} and b denote the maximum adsorption capacity of adsorbents (mg g^{-1}) and Langmuir adsorption constant (L mg^{-1}). q_{max} and b can be calculated from the slope and intercept of the linear plots of C_e/q_e against C_e (Figure 6).

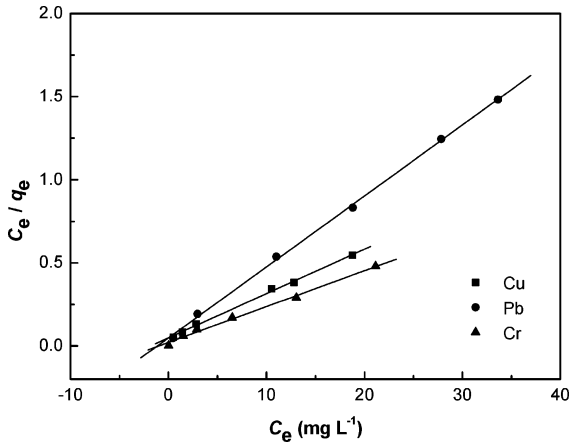

Figure 6. Langmuir adsorption isotherm plots for the adsorption of Cu(II), Pb(II), and Cr(III) onto G−ZnO composites. Dosage of adsorbent = 0.02 g, concentration of metal ions = 10 mg L^{-1}, contact time = 120 min, pH = 6.0.

Langmuir isotherm can be described by a dimensionless constant called equilibrium parameter, R_L, which is usually defined by

$$R_L = \frac{1}{1 + bC_0} \quad (6)$$

where C_0 denotes the highest initial concentration of metal ions (mg L^{-1}) and b is the Langmuir constant that indicates the nature of adsorption. The value of R_L indicates that the type of the adsorption isotherm is either $R_L > 1$, $R_L = 1$, $0 < R_L < 1$, or

Table 1. Kinetic Parameters for the Adsorption of Cu(II), Pb(II), and Cr(III) onto G−ZnO Composites

		pseudo-first-order			pseudo-second-order		
metal	$q_{e,exp}$ mg g^{-1}	k_1	$q_{e,cal}$ mg g^{-1}	R^2	k_2	$q_{e,cal}$ mg g^{-1}	R^2
Cu(II)	9.98	0.066	17.27	0.8524	0.104	9.72	0.9963
Pb(II)	8.65	0.017	8.14	0.4007	0.382	8.18	0.9871
Cr(III)	9.70	0.005	1.68	0.2838	0.331	9.57	0.9972

dx.doi.org/10.1021/je400384z | J. Chem. Eng. Data 2013, 58, 2395−2401

$R_L = 0$, while the metal ions are favorable for the adsorption at $0 < R_L < 1$.[41]

The Freundlich isotherm model is considered as the adsorption which occurs on a heterogeneous surface with uniform energy. It can be represented as follows,

$$\log q_e = \frac{1}{n}\log C_e + \log K \quad (7)$$

where K and n are the Freundlich constants, which denote the adsorption capacity and the adsorption strength, respectively. K and n can be calculated from the intercept and the slope of the linear plots of log q_e versus log C_e.

The results obtained from the two adsorption isotherms were shown in Table 2. By a comparison of the R^2 values of both models, the Langmuir model fit the experimental data better, suggesting the monolayer adsorption of Cu(II), Pb(II), and Cr(III) onto the surface of the G−ZnO composites. Furthermore, the values of the dimensionless parameter, R_L, are between 0.023 and 0.034 ($0 < R_L < 1$), which is consistent with the requirement for a favorable adsorption process.

Table 2. Parameters of the Langmuir and Freundlich Isotherms for Cu(II), Pb(II), and Cr(III) Adsorption

	Langmuir model			
metal	q_{max}/mg g^{-1}	b/L mg^{-1}	R_L	R^2
Cu(II)	37.45	0.55	0.034	0.9975
Pb(II)	23.42	0.87	0.025	0.9990
Cr(III)	46.30	0.99	0.023	0.9942
	Freundlich model			
metal	n	k	R^2	
Cu(II)	2.90	13.59	0.9722	
Pb(II)	4.97	11.93	0.9736	
Cr(III)	4.17	22.92	0.9823	

The comparison of the maximum adsorption capacity of Cu(II), Pb(II), and Cr(III) with various adsorbents was listed in Table 3. It can be seen that G−ZnO composites have a relatively large adsorption capacity of 37.45, 23.42, and 46.30 mg g^{-1} for Cu(II), Pb(II), and Cr(III), respectively, indicating that G−ZnO is a potential material for removal of Cu(II), Pb(II), and Cr(III) from aqueous solutions.

Table 3. Comparison of Maximum Adsorption Capacities (mg g^{-1}) with Various Adsorbents for Cu(II), Pb(II), and Cr(III)

adsorbents	Cu(II)	Pb(II)	Cr(III)	ref
nanometer-size TiO_2	26.50			17
kaolin	0.76	0.66	1.81	42
celtek clay		18.08	21.55	43
acid functionalized multiwalled carbon nanotubes	6.64	8.98		44
chitosan/attapulgite composites			27.03	45
amino-functionalized magnetic nanoadsorbent	12.43			46
activated carbon prepared from coconut shell		26.50		47
G−ZnO composites	37.54	23.42	46.30	this work

3.7. Thermodynamic Parameters of Adsorption. The changes of enthalpy (ΔH), entropy (ΔS), and Gibbs free energy (ΔG), were calculated to predict the process of adsorption. These thermodynamic parameters could be obtained as follows:

$$K_d = \frac{q_e}{C_e} \quad (8)$$

$$\Delta G = -RT \ln K_d \quad (9)$$

$$\ln K_d = \frac{\Delta S}{R} - \frac{\Delta H}{RT} \quad (10)$$

where K_d is the thermodynamic equilibrium constant, R (8.3145 J mol^{-1} K^{-1}) is the ideal gas constant, and T (K) is the absolute temperature. ΔH and ΔS were calculated from the slopes and intercepts of the plot of ln K_d vs $1/T$ by using eq 10.

In this work, effects of experimental temperatures on the adsorption were investigated in the range of 20−40 °C when other parameters (pH values, adsorbent dosage, and metal ion concentration) were kept constant. Results of thermodynamic parameters were illustrated in Table 4. The negative values of ΔG for all the three metals show that the adsorption processes are spontaneous. The positive values of ΔH indicate the endothermic behavior of the adsorption. The positive value of ΔS reflects the increasing randomness at the solid/solution interface during the adsorption process. The thermodynamic parameters are actually favorable in the practical application of the process.

Table 4. Thermodynamic Parameters for the Adsorption of Cu(II), Pb(II), and Cr(III) onto G−ZnO Composites

metal	T/K	$\Delta G°$/kJ mol^{-1}	$\Delta H°$/kJ mol^{-1}	$\Delta S°$/J mol^{-1} K^{-1}
Cu(II)	293	−6.842	2.447	0.0317
	303	−7.161		
	313	−7.476		
Pb(II)	293	−5.493	24.723	0.1032
	303	−6.621		
	313	−7.254		
Cr(III)	293	−10.376	11.734	0.0755
	303	−11.164		
	313	−11.884		

3.8. Recycling Study of G−ZnO Composites. As a representative, Cu(II) was studied for the recycling experiments. After the adsorption process finished, the loaded G−ZnO composites were sequentially treated with 0.1 mol L^{-1} HCl and deionized water for the goal of regeneration. Through these simple processes, the adsorbed Cu(II) was washed out and the G−ZnO composites were regenerated. The adsorption percentage of Cu(II) with G−ZnO composites remained above 95 % after three times of recycling test (98.6 % for n = 1, 97.8 % for n = 2, and 95.1% for n = 3). Results of the recovery tests indicated that G−ZnO composites can be employed as a kind of recyclable adsorbents for the removal of heavy metal ions.

4. CONCLUSIONS

In the present study, G−ZnO composites were prepared and employed for the adsorption of metal ions. The composites showed good performance for the removal of Cu(II), Pb(II), and Cr(III) from aqueous solutions. Effects of pH and contact time were studied in batch experiments. Kinetics, adsorption isotherms, and thermodynamics were also examined. The kinetics study revealed that adsorption rate is fast and fit a pseudo-second-order model. The Langmuir and Freundlich isotherm models for Cu(II), Pb(II), and Cr(III) onto G−ZnO composites were studied, demonstrating that the Langmuir model fit the adsorption data better. Thermodynamic

parameters suggested that the adsorption process is a spontaneous and endothermic one. Because of the high adsorption capacity and short equilibrium time, G−ZnO composites have the potential for removal of heavy metals in solutions.

AUTHOR INFORMATION

Corresponding Author

*E-mail: jiaqiong@jlu.edu.cn.

Funding

The project was supported by State Key Laboratory of Inorganic Synthesis and Preparative Chemistry, College of Chemistry, Jilin University (2012−16).

Notes

The authors declare no competing financial interest.

REFERENCES

(1) Soylak, M.; Erdogan, N. D. Copper(II)-rubeanic acid coprecipitation system for separation-preconcentration of trace metal ions in environmental samples for their flame atomic absorption spectrometric determinations. *J. Harzard. Mater.* **2006**, *137*, 1035−1041.

(2) Uluozlu, O. D.; Tuzen, M.; Mendil, D.; Soylak, M. Coprecipitation of trace elements with Ni^{2+}/2-Nitroso-1-naphthol-4-sulfonic acid and their determination by flame atomic absorption spectrometry. *J. Harzard. Mater.* **2010**, *176*, 1032−1037.

(3) Bessbousse, H.; Rhlalou, T.; Verchere, J. F.; Lebrun, L. Removal of heavy metal ions from aqueous solutions by filtration with a novel complexing membrane containing poly(ethyleneimine) in a poly(vinyl alcohol) matrix. *J. Membr. Sci.* **2008**, *307*, 249−259.

(4) Kumbasar, R. A. Selective extraction and concentration of chromium(VI) from acidic solutions containing various metal ions through emulsion liquid membranes using Amberlite LA-2. *J. Ind. Eng. Chem.* **2010**, *16*, 829−836.

(5) Verma, V. K.; Tewari, S.; Rai, J. P. N. Ion exchange during heavy metal bio-sorption from aqueous solution by dried biomass of macrophytes. *Bioresour. Technol.* **2008**, *99*, 1932−1938.

(6) Tu, Z. F.; He, Q.; Chang, X. J.; Hu, Z.; Gao, R.; Zhang, L. N.; Li, Z. H. 1-(2-Formamidoethyl)-3-phenylurea functionalized activated carbon for selective solid-phase extraction and preconcentration of metal ions. *Anal. Chim. Acta* **2009**, *649*, 252−257.

(7) da Silva, E. L.; Martins, A. O.; Valentini, A.; de Favere, V. T.; Carasek, E. Application of silica gel organofunctionalized with 3(1-imidazolyl)propyl in an on-line preconcentration system for the determination of copper by FAAS. *Talanta* **2004**, *64*, 181−189.

(8) Huang, C. Z.; Jiang, Z. C.; Hu, B. Mesoporous titanium dioxide as a novel solid-phase extraction material for flow injection micro-column preconcentration on-line coupled with ICP−OES determination of trace metals in environmental samples. *Talanta* **2007**, *73*, 274−281.

(9) Mahmoud, M. E.; Osman, M. M.; Hafez, O. F.; Elmelegy, E. Removal and preconcentration of lead (II), copper (II), chromium (III) and iron (III) from wastewaters by surface developed alumina adsorbents with immobilized 1-nitroso-2-naphthol. *J. Harzard. Mater.* **2010**, *173*, 349−357.

(10) Moradi, O.; Aghaie, M.; Zare, K.; Monajjemi, M.; Aghaie, H. The study of adsorption characteristics Cu^{2+} and Pb^{2+} ions onto PHEMA and P(MMA-HEMA) surfaces from aqueous single solution. *J. Harzard. Mater.* **2009**, *170*, 673−679.

(11) Segatelli, M. G.; Santos, V. S.; Presotto, A. B. T.; Yoshida, I. V. P.; Tarley, C. R. T. Cadmium ion-selective sorbent preconcentration method using ion imprinted poly(ethylene glycol dimethacrylate-*co*-vinylimidazole). *React. Funct. Polym.* **2010**, *70*, 325−333.

(12) Duran, C.; Gundogdu, A.; Bulut, V. N.; Soylak, M.; Elci, L.; Senturk, H. B.; Tufekci, M. Solid-phase extraction of Mn(II), Co(II), Ni(II), Cu(II), Cd(II) and Pb(II) ions from environmental samples by flame atomic absorption spectrometry (FAAS). *J. Harzard. Mater.* **2007**, 347−355.

(13) Tuzen, M.; Saygi, K. O.; Soylak, M. Solid phase extraction of heavy metal ions in environmental samples on multiwalled carbon nanotubes. *J. Harzard. Mater.* **2008**, *152*, 632−639.

(14) Rao, G. P.; Lu, C.; Su, F. Sorption of divalent metal ions from aqueous solution by carbon nanotubes: A review. *Sep. Purif. Technol.* **2007**, *58*, 224−231.

(15) Henglein, A. Small-particle research: physicochemical properties of extremely small colloidal metal and semiconductor particles. *Chem. Rev.* **1989**, *89*, 1861−1873.

(16) Engates, K. E.; Shipley, H. J. Adsorption of Pb, Cd, Cu, Zn, and Ni to titanium dioxide nanoparticles: effect of particle size, solid concentration, and exhaustion. *Environ. Sci. Pollut. Res.* **2011**, *18*, 386−395.

(17) Qian, S. H.; Zhang, S. J.; Huang, Z.; Xiao, M.; Huang, F. Preconcentration of ultra-trace copper in water samples with nanometer-size TiO_2 colloid and determination by GFAAS with slurry sampling. *Microchim. Acta* **2009**, *166*, 251−254.

(18) Uheida, A.; Salazar-Alvarez, G.; Bjorkman, E.; Yu, Z.; Muhammed, M. Fe_3O_4 and γ-Fe_2O_3 nanoparticles for the adsorption of Co^{2+} from aqueous solution. *J. Colloid Interface Sci.* **2006**, *298*, 501−507.

(19) Mayo, J. T.; Yavuz, C.; Yean, S.; Cong, L.; Shipley, H.; Yu, W.; Falkner, J.; Kan, A.; Tomson, M.; Colvin, V. L. The effect of nanocrystalline magnetite size on arsenic removal. *Sci. Techonl. Adv. Mater.* **2007**, *8*, 71−75.

(20) Hristovski, K.; Baumgardner, A.; Westerhoff, P. Selecting metal oxide nanomaterials for arsenic removal in fixed bed columns: From nanopowders to aggregated nanoparticle media. *J. Harzard. Mater.* **2007**, *147*, 265−274.

(21) Kikuchi, Y.; Qian, Q. R.; Machida, M.; Tatsumoto, H. Effect of ZnO loading to activated carbon on Pb(II) adsorption from aqueous solution. *Carbon* **2006**, *44*, 195−202.

(22) Zhang, S. J.; Li, X. Y.; Chen, J. P. Preparation and evaluation of a magnetite-doped activated carbon fiber for enhanced arsenic removal. *Carbon* **2010**, *48*, 60−67.

(23) Chen, C. L.; Hu, J.; Shao, D. D.; Li, J. X.; Wang, X. K. Adsorption behavior of multiwall carbon nanotube/iron oxide magnetic composites for Ni(II) and Sr(II). *J. Harzard. Mater.* **2009**, *164*, 923−928.

(24) Miyamoto, J.; Kanoh, K.; Kaneko, K. The addition of mesoporosity to activated carbon fibers by a simple reactivation process. *Carbon* **2005**, *43*, 855−857.

(25) Zhao, X. W.; Jia, Q.; Song, N. Z.; Zhou, W. H.; Li, Y. S. Adsorption of Pb(II) from an aqueous solution by titanium dioxide/carbon nanotube nanocomposites: kinetics, thermodynamics, and isotherms. *J. Chem. Eng. Data* **2010**, *55*, 4428−4433.

(26) Di, Z. C.; Ding, J.; Peng, X. J.; Li, Y. H.; Luan, Z. K.; Liang, J. Chromium adsorption by aligned carbon nanotubes supported ceria nanoparticles. *Chemosphere* **2006**, *62*, 861−865.

(27) Narin, I.; Soylak, M.; Kayakirilmaz, K.; Elci, L.; Dogan, M. Preparation of a chelating resin by immobilizing 1-(2-pyridylazo) 2-naphtol on Amberlite XAD-16 and its application of solid phase extraction of Ni(II), Cd(II), Co(II), Cu(II), Pb(II), and Cr(III) in natural water samples. *Anal. Lett.* **2003**, *36*, 641−658.

(28) Novoselov, K. S.; Geim, A. K.; Morozov, S. V.; Jiang, D.; Zhang, Y.; Dubonos, S. V.; Grigorieva, I. V.; Firsov, A. A. Electric field effect in atomically thin carbon films. *Science* **2004**, *306*, 666−669.

(29) Chandra, V.; Park, J.; Chun, Y.; Lee, J. W.; Hwang, I. C.; Kim, K. S. Water-dispersible magnetite-reduced graphene oxide composites for arsenic removal. *ACS Nano* **2010**, *4*, 3979−3986.

(30) Stankovich, S.; Dikin, D. A.; Dommett, G. H. B.; Kohlhaas, K. M.; Zimney, E. J.; Stach, E. A.; Piner, R. D.; Nguyen, S. T.; Ruoff, R. S. Graphene-based composite materials. *Nature* **2006**, *442*, 282−286.

(31) Xu, Y. X.; Bai, H.; Lu, G. W.; Li, C.; Shi, G. Q. Flexible graphene films via the filtration of water-soluble noncovalent functionalized graphene sheets. *J. Am. Chem. Soc.* **2008**, *130*, 5856−5857.

(32) Flytzani-Stephanopoulos, M.; Sakbodin, M.; Wang, Z. Regenerative adsorption and removal of H_2S from hot fuel gas streams by rare earth oxides. *Science* **2006**, *9*, 1508−1510.

(33) Wang, X. B.; Cai, W. P.; Lin, Y. X.; Wang, G. Z.; Liang, C. H. Mass production of micro/nanostructured porous ZnO plates and their strong structurally enhanced and selective adsorption performance for environmental remediation. *J. Mater. Chem.* **2010**, *20*, 8582−8590.
(34) Hummers, W.; Offeman, R. Preparation of graphitic oxide. *J. Am. Chem. Soc.* **1958**, *80*, 1339−1340.
(35) Kovtyukhova, N. I.; Ollivier, P. J.; Martin, B. R.; Mallouk, T. E.; Chizhik, S. A.; Buzaneva, E. V.; Gorchinskiy, A. D. Layer-by-layer assembly of ultrathin composite films from micron-sized graphite oxide sheets and polycations. *Chem. Mater.* **1999**, *11*, 771−778.
(36) Zou, W. B.; Zhu, J. W.; Sun, Y. X.; Wang, X. Depositing ZnO nanoparticles onto graphene in a polyol system. *Mater. Chem. Phys.* **2011**, *125*, 617−620.
(37) Nakajima, T.; Mabuchi, A.; Hagiwara, R. A new structure model of graphite oxide. *Carbon* **1988**, *26*, 357−361.
(38) Cai, D. Y.; Song, M. Preparation of fully exfoliated graphite oxide nanoplatelets in organic solvents. *J. Mater. Chem.* **2007**, *17*, 3678−3680.
(39) Schniepp, H. C.; Li, J. L.; McAllister, M. J.; Sai, H.; Herrera-Alonso, M.; Adamson, D. H.; Prud'homme, R. K.; Car, R.; Saville, D. A.; Aksay, I. A. Functionalized single graphene sheets derived from splitting graphite oxide. *J. Phys. Chem. B* **2006**, *110*, 8535−8539.
(40) Ho, Y. S.; McKay, G. Pseudo-second order model for sorption processes. *Process Biochem.* **1999**, *34*, 451−465.
(41) Ramesh, A.; Hasegawa, H.; Sugimoto, W.; Maki, T.; Ueda, K. Adsorption of gold(III), platinum(V) and palladium(II) onto glycine modified crosslinked chitosan resin. *Bioresour. Technol.* **2008**, *99*, 3801−3809.
(42) Chantawong, V.; Harvey, N. W.; Bashkin, V. N. Comparison of heavy metal adsorptions by thai kaolin and ballclay. *Water Air Soil Pollut.* **2003**, *148*, 111−125.
(43) Sar, A.; Tuzen, M.; Soylak, M. Adsorption of Pb(II) and Cr(III) from aqueous solution on Celtek clay. *J. Harzard. Mater.* **2007**, *144*, 41−46.
(44) Wang, J. P.; Ma, X. X.; Fang, G. Z.; Pan, M. F.; Ye, X. K.; Wang, S. Preparation of iminodiacetic acid functionalized multi-walled carbon nanotubes and its application as sorbent for separation and preconcentration of heavy metal ions. *J. Harzard. Mater.* **2011**, *186*, 1985−1992.
(45) Zou, X. H.; Pan, J. M.; Ou, H. X.; Wang, X.; Guan, W.; Li, C. X.; Yan, Y. S.; Duan, Y. Q. Adsorptive removal of Cr(III) and Fe(III) from aqueous solution by chitosan/attapulgite composites: Equilibrium, thermodynamics and kinetics. *Chem. Eng. J.* **2011**, *167*, 112−121.
(46) Huang, S. H.; Chen, D. H. Rapid removal of heavy metal cations and anions from aqueous solutions by an amino-functionalized magnetic nano-adsorbent. *J. Harzard. Mater.* **2009**, *163*, 174−179.
(47) Sekar, M.; Sakthi, V.; Rengaraj, S. Kinetics and equilibrium adsorption study of lead(II) onto activated carbon prepared from coconut shell. *J. Colloid Interface Sci.* **2004**, *279*, 307−313.